QUANTUM CONFINED STARK EFFECT IN INGAAS/INP AND INGAAS/INGAASP MULTI QUANTUM WELL STRUCTURES

T. Tütken, G. Frankowsky, A. Hangleiter,
V. Härle, K. Streubel, F. Scholz
4. Physikalisches Institut, Universität Stuttgart
Pfaffenwaldring 57
D-7000 Stuttgart 80
Federal Republic of Germany

(Received 1 August 1990)

Differential electrotransmission measurements on InGaAs/InP and InGaAs/InGaAsP multi quantum well structures (MQW) with well widths 8,10 and 20 nm with InGaAsP barriers of $E_g(77K) = 1.2\,eV$ are presented. The differential electrotransmission spectra were fitted with a lorentzian lineshape model for the excitonic transition. A Stark shift of up to 18 meV was observed for the 8 nm InGaAs/InGaAsP quantum well structure. The results were compared to a calculation of the Stark effect including the field dependent exciton binding energy. We find good agreement between experiment and theory. The well width dependence of the oscillator strength shows a maximum for $L_z = 11\,nm$ when changing the field from $1 \cdot 10^4 V/cm$ to $1 \cdot 10^5 V/cm$.

1. Introduction

The loss minimum of optical fibers at $1.3-1.5\mu m$ favors InGaAs(P)/InP as material for optoelectronic purposes like lasers [1] and modulators. Changing the composition in InGaAsP allows to achieve a wide range of bandgaps for barrier material or even well material for quantum well devices. The change in the layer thickness of the quantum well material changes also the position of the lowest optical transition.

An external optical modulator for semiconductor lasers based on the quantum confined Stark effect for a quantum well laser should avoid the high frequency chirp of current modulated lasers. Using InGaAsP as confining structure for the quantum well packet allows to build a waveguide based on the change of refractive index between InGaAsP and the InP substrate and contact layer. The reduced height of the barriers for the electrons and holes should have an influence on the change of energy levels and oscillator strength.

In this paper we study multi quantum well (MQW) structures with InGaAs wells and barriers of InGaAsP with a band gap of $\approx 1.2\,eV$ at $2\,K$ lattice matched to InP at growth temperature and compare the results with an InGaAs/InP MQW structure. We investigate the quantum confined Stark effect in our structures with differential electrotransmission measurements at $77\,K$. The spectra were fitted with a lineshape model for the excitonic transition. The resulting line position, and intensity where compared with calculation of the energy shift and oscillator strength of the excitonic line.

2. Investigated Structures

The quantum well structures were grown by low pressure metal organic chemical vapor deposition (MOCVD) on Sulfur doped InP substrate with a doping level of $1.2 \cdot 10^{19}\,cm^{-3}$. A undoped InP buffer layer (330 nm) was grown prior to the InGaAsP confinement layer of 160 nm followed by the multi quantum well packet with 10 InGaAs wells separated by 16 nm InGaAsP barriers. In the case of the 20 nm MQW structure only 3 periods are grown and the InP buffer on the substrate was Sulfur doped with $n = 3 \cdot 10^{17}\,cm^{-3}$ at $77K$. We choose broad barriers of 16 nm to decouple the wells since a coupling of the wells would lead to a splitting of the energy levels and a broadening of the optical transitions [2].

After the second confinement layer (16 nm InGaAsP) an undoped InP spacer layer of 80 nm was grown. On top of this structure a contact layer of 1.5 μm InP Zn doped of a level of $3 \cdot 10^{17}\,cm^{-3}$ was grown. Stan-

0749-6036/90/040309+05 $02.00/0

dard ohmic contacts were made on the substrate and the contact layer. Furthermore a structure with 20 × 10 nm InGaAs wells separated by 30 nm InP barriers was investigated. In this case the electric top contact was a 7 nm thick gold Schottky contact. The well width of the 10 nm and the 20 nm InGaAsP MQW structures has been checked with a high resolution scanning electron microscope.

The 2 K luminescence of the InGaAsP structures reveals a linewidth of 15 to 17 meV at low excitation with a Nd:YAG laser. The luminescence of the InGaAs/InP structure shows a linewidth of 7 meV. The absorption spectra at 2 K of the 8 and 10 nm InGaAs/InGaAsP and the 10 nm InGaAs/InP sample show an excitonic enhancement of the absorption edge.

3. Calculation of the Energy Levels under electric Field

The broad barriers allow us to treat the whole MQW in the calculation as a single quantum well. The small barrier height of $\approx 170meV$ for the electrons made it necessary to use a resonant method [3] to calculate the energy levels and wavefunctions. The energy level for the more confined heavy holes were calculated using the standard transfer matrix method [4]. Knowing the wavefunctions we have calculated the exciton binding energy. The Hamilton operator H_{ex} for a excitons in a quantum well of well width L_z in an electric field F in the envelope function formalism can be split into three contributions [5]. H_{ez}, H_{hz} are the Hamilton operators for electrons and holes depending on the corresponding effective masses m_e, m_h [6,7] and potentials V_e, V_h. The conduction band discontinuity has been taken as 39 % [8]. For the calculation of the exciton binding energy E_{eb} we used an averaged dielectric constant $\epsilon = 13.0$ [9] and calculated the reduced mass μ with the masses of the well material.

$$
\begin{aligned}
H_{ex} &= H_{ez} + H_{hz} + H_{eb} \\
H_{ez} &= \frac{-\hbar^2}{2m_e}\frac{\partial^2}{\partial z_e^2} + V_e(z_e) + eFz_e \\
H_{hz} &= \frac{-\hbar^2}{2m_h}\frac{\partial^2}{\partial z_h^2} + V_h(z_h) - eFz_h \\
H_{eb} &= \frac{-\hbar^2}{2\mu}\frac{\partial^2}{\partial r^2} - \frac{e^2}{\epsilon[(z_e - z_h)^2 + r^2]^{1/2}}
\end{aligned}
$$

The exact solution for the Hamilton operator H_{ez} and H_{hz} in the quantum well and in the barrier are the Airy functions Ai, Bi. The boundary condition between regions of different potential and effective masses were realized with the transfer matrix method assuming continuous flux and wavefunction across the boundary. The wavefunction has been normalised within the effective well width l_{eff} at zero field.

$$l_{eff} = \frac{\pi\hbar}{2mE_z}$$

m is the effective mass of the carrier and E_z is the quantisation energy. Using the wavefunctions Ψ_e, Ψ_h for electrons and holes it is possible to calculate the exciton binding energy using the assumption of a separable $1s$ - like wave function for the exciton.

$$\Phi_{ex}(z_e, z_h, r) = \Psi_e(z_e) \cdot \Psi_h(z_h) \cdot \sqrt{\frac{2}{\pi}}\frac{\exp(-r/R_{ex})}{R_{ex}}$$

Varying the exciton radius R_{ex} leads to minimum in the exciton binding energy E_{ex} which must be subtracted from the quantisation energies of the electron and the hole. The oscillator strength f due to the $1ehh$ exciton can be calculated by the equation [10]

$$f = \frac{Q^2}{2\pi m_0 E_{ex} R_{ex}^2 L_z}\left|\int_{-\infty}^{\infty} \Psi_e(z) \cdot \Psi_h(z)dz\right|$$

where Q is the momentum matrix element. The absorption resulting from this oscillator strength is given by

$$\alpha(E, F) = \frac{4\pi^2 e^2 \hbar}{n m_0 c} f(F) \cdot g(E)$$

where n is the refractive index and $g(E)$ is the lineshape for the $1ehh$ excitonic transition. For a good modulation on/off ratio it is necessary to get a change of the absorption at a specific energy which can be due to a change in oscillator strength and/or a shift in the energy position of the excitonic transition.

4. Results of the Calculations

The total change of the energy position of the $1ehh$ excitonic transition depends strongly on the well width (Fig. 1). We calculated an increase of the energy position for well widths smaller than $\approx 20\,nm$ when increasing the field from $7 \cdot 10^4 V/cm$. The wavefunction of the electron leaks out of the well even at low fields leading to a broadening of the transition. Thus it may not be possible to experimentally verify this effect. The more the well width is enlarged the more the total energy shift grows (Fig. 1). For all well widths considered the contribution of the excitonic binding energy to the total energy shift is below $2\,meV$ in the range from $1 \cdot 10^4 V/cm$ to $1 \cdot 10^5\ V/cm$ (Fig. 1). The excitonic binding energy goes down with increasing well width because of the larger carrier separation in the broader wells. The field dependence of the oscillator strength is mainly dominated by the change of the overlap between electron and hole wavefunctions. The L_z dependence shows a maximum for $L_z = 11\ nm$ when changing the field from $1 \cdot 10^4 V/cm$ to $1 \cdot 10^5 V/cm$ (Fig. 2).

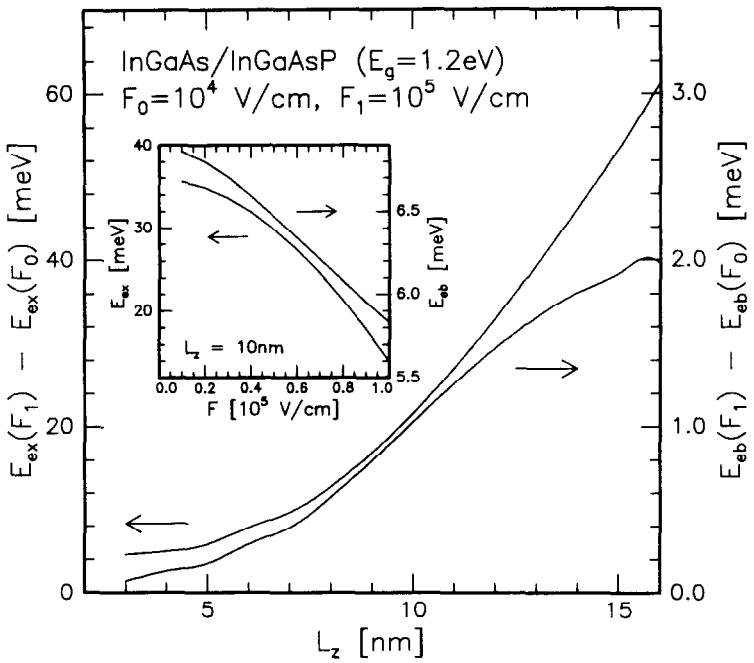

Fig. 1 : Calculated change of excitonic binding energy E_{eb} and the total excitonic transition energy E_{ex} by a change of the electric field from $1 \cdot 10^4\, V/cm$ to $1 \cdot 10^5\, V/cm$ for a InGaAs single quantum well in InGaAsP ($E_g = 1.2\, eV$). Inset showing the field dependence of these quantities for a $10\, nm$ well.

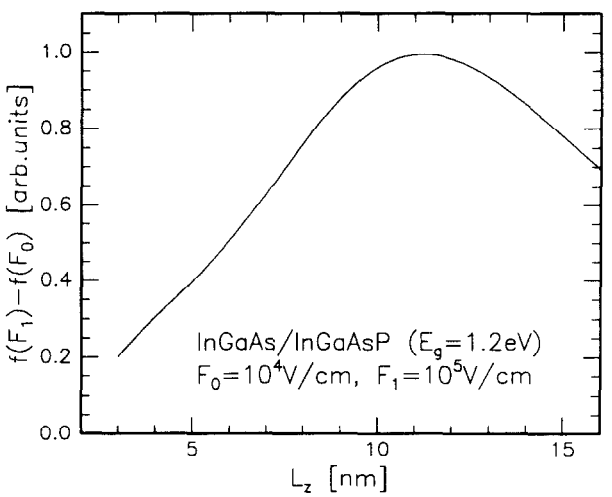

Fig. 2 : Calculated L_z dependence of the oscillator strength f by a change of the electric field from $1 \cdot 10^4\, V/cm$ to $1 \cdot 10^5\, V/cm$ for a InGaAs single quantum well in InGaAsP ($E_g = 1.2\, eV$).

5. Differential Electrotransmission Measurements

Differential transmission spectra perpendicular to the quantum well structure were measured using standard lock-in technique. The current density through the structure was always below $0.05\,mA/mm$.

The resulting spectra show two different features : 1) the quantum confined Stark effect from the InGaAs wells 2) the Franz-Keldysh effect from the barrier material.

A lorentzian lineshape of the exciton in the absorption spectra at constant voltage results in a difference of two lorentzian lines in the differential transmission spectrum. We fitted the low energy side of the Stark effect signal with a difference of two lorentzian lines for the $1ehh$ and $1elh$ excitonic transition. The results of such a fit are the line position, intensity, width and the modulation of the line position at the corresponding offset voltage. At high voltages it was possible to fit the spectra with only one excitonic line (Fig. 3). At high voltages the splitting between $1ehh$ and the $1elh$ excitonic transition increases so it is easier to resolve the lowest transition.

For the structure with $10\,nm$ wells in InGaAsP we observe a shift of $15\,meV$ in the voltage range between $+0.6\,V$ and $-4.4\,V$. The structure with the $8\,nm$ wells in InGaAsP shows a shift of about $18\,meV$ in the range between $+0.8\,V$ and $-7.0\,V$. In the $20\,nm$ well we were able to resolve two low energy transitions. The lowest transition is smaller and vanishes when applying negative voltages. The lowest transition in the InGaAs/InP structure shows a shift of $10\,meV$ in the range between $0\,V$ and $-6.8\,V$.

The fitted linewidth at low fields of the exciton agrees well with the linewidth of the low temperature luminescence.

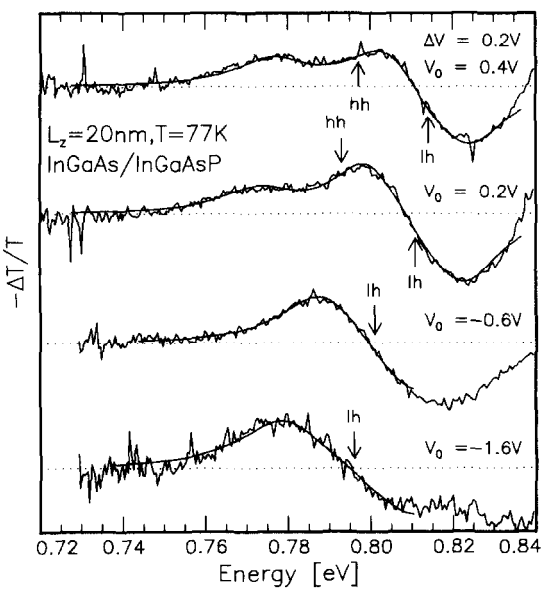

Fig. 3 : Differential transmission spectrum for the $20\,nm$ InGaAs/InGaAsP MQW with fit. The arrows are indicating the fitted line positions.

6. Comparison of Differential Transmission Measurements with Calculations

The calculations give as a result the shift of the $1ehh$ transition versus the electric field applied to the quantum well. The applied voltage was transformed into the electric field just by dividing by the width of the undoped structure adding the field due to the alignment of the Fermi level of the substrate and the contact layer.

The only free parameter for the theoretical curves was the band gap for the InGaAs well which differs for the $10\,nm$ InGaAs/InP and the $8\,nm$ InGaAs/InGaAsP samples in the range of $15\,meV$ from the value of $0.80\,eV$. This could be explained with composition changes in the InGaAs well.

As seen in figure 4 we get a good agreement between the calculations and the shift of the lowest transition fit-

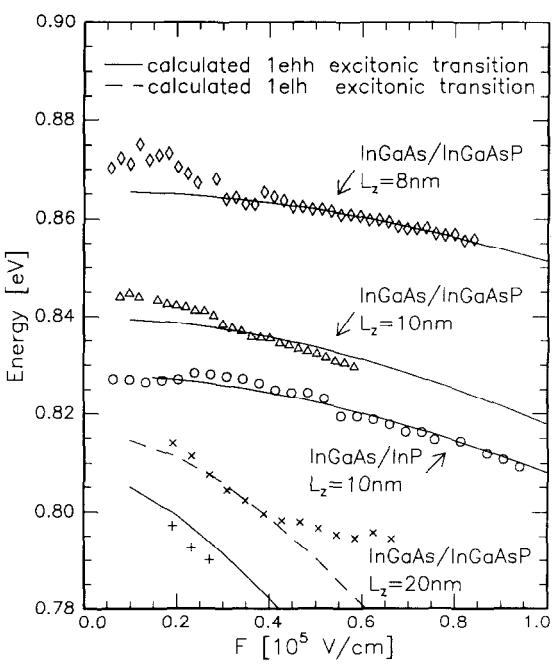

Fig. 4 : Comparison between fitted line position and calculated energy shift. We added bandgap energy of 0.818, 0.800, $0.804\,eV$ to the calculations of the energy shift for the 8, 10, $20\,nm$ InGaAs/InGaAsP MQW structures and $0.798\,eV$ for the $10\,nm$ InGaAs/InP MQW.

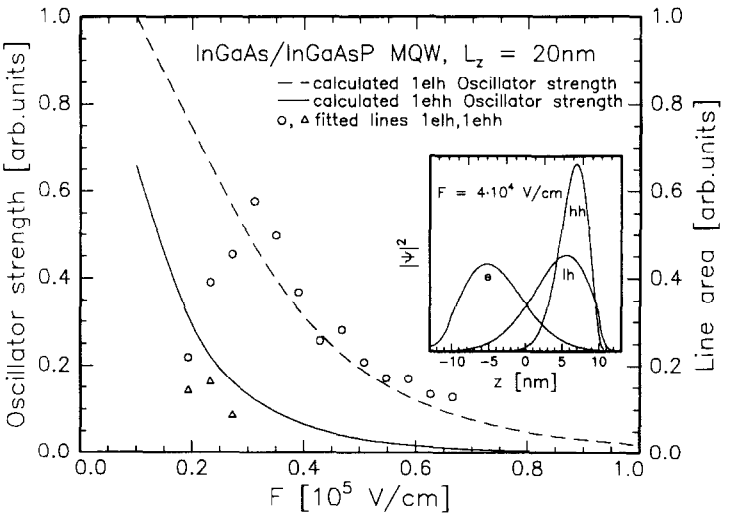

Fig. 5 : Comparison of the area of the fitted excitonic line with the calculated oscillator strength for the 20 nm InGaAs/InGaAsP MQW. Inset showing corresponding wavefunctions at $4 \cdot 10^4\, V/cm$.

ted from the experimental data for all MQW structures. We observed the largest differential change in energy for the widest wells.

In the case of the 20 nm sample it was possible to resolve the 1ehh and the 1elh transition. An elastic strain of $\epsilon = 1 \cdot 10^{-3}$ [11] could explain the deviation in the difference of the 1elh to 1ehh splitting between theory and experiment. The vanishing intensity of the 1ehh transition compared to the 1elh transition could be explained with the difference in the change of the oscillator strength for both transitions (Fig. 5).

7. Conclusions

We observed a Stark shift of excitonic transitions in InGaAs/InGaAsP for well widths of 8,10 and 20 nm and compared these data with measurements on a 10 nm InGaAs/InP multi quantum well structure. The experimental results could be analysed by fitting the differential absorption spectra. The resulting line positions agree well with the results of calculations of the excitonic shift. The change of the excitonic binding energy is only a small contribution to the total shift. In the 20 nm well we resolved the 1elh and the 1ehh transition. The 10 nm InGaAs/InP MQW shows a smaller energy shift as the InGaAs/InGaAsP MQW of the same well width which agrees with the results of our calculations. Reducing the band gap of the InGaAsP material would enlarge the difference in favor for the InGaAs/InGaAsP material. The well width dependence of the oscillator strength for 1ehh exciton shows a maximum for $L_z = 11\, nm$, when changing the field from $1 \cdot 10^4 V/cm$ to $1 \cdot 10^5 V/cm$.

References

1 G.P.Agraval and N.K.Dutta, Long wavelength semiconductor lasers, Van Nostrand (1986)

2 G.Fuchs, J.Hörer, and A.Hangleiter , to be published

3 E.J.Austin and M.Jaros, Physical Review B **31** (8), 5569 (1985)

4 W.W.Lui and M.Fukuma, Journal of Applied Physics **60** (5), 1555 (1986)

5 D.A.B.Miller, D.S.Chemla, T.C.Damen, A.C. Gossard, and W.Wiegmann, T.H.Wood and C.A. Burrus, Physical Review B **53** (22), 2173 (1984)

6 R.J.Nicholas, J.C.Portal, C.Houlbert, P.Pierrier, and T.P.Pearsall, Applied Physics Letters **34**, 492 (1979)

7 P.Lawaetz, Physical Review **134**, 3460 (1971)

8 S.R.Forrest, P.H.Schmidt, R.B.Wilson, and M.L. Kaplan, Applied Physics Letter, **45**, 1199 (1984)

9 S.Adachi, Journal of Applied Physics **53** (12), 8775 (1982)

10 K.N.Bhi and T.Hiroschina, Applied Physics Letters **51**, 320 (1987)

11 C.P.Kuo, S.K.Vong, R.M.Cohen, and G.B. Stringfellow, Journal of Applied Physics **57** (12), 5428 (1985)